

## Probing the photoelectrochemical performance of spray-coated $\text{Cu}_2\text{CoSnS}_4$ thin films on FTO substrate

P.S. Maldar\*, S.N. Pusawale, A.S. Tambat

Rajarambapu Institute of Technology, Affiliated to Shivaji University Kolhapur,  
Rajaramnagar, Islampur, Maharashtra 415414, India

\*Corresponding author e-mail: parvezmaldar8@gmail.com

**Abstract.** This research reports the deposition of fluorine-doped tin oxide (FTO) thin films, which were used as conducting electrodes for the deposition of  $\text{Cu}_2\text{CoSnS}_4$  (CCTS) thin films, with an indigenously designed spray pyrolysis setup. Both FTO and CCTS thin films have been deposited using the chemical spray pyrolysis method. The CCTS thin films were deposited with a constant quantity of the precursor solution of 80 ml. The deposition temperature was 350 °C for CCTS thin films, and the ratio of cations to anions was 1:7 in the precursor solution. The deposited CCTS thin films were studied using X-ray diffraction, scanning electron microscopy, and Raman spectroscopy. Additionally, the photoactivity study was carried out. It was obtained that the efficiency of photoelectrochemical solar cells fabricated with a thiourea concentration of 1:7 for cations is 2.33%.

**Keywords:** photoelectrochemical cell, FTO thin films,  $\text{Cu}_2\text{CoSnS}_4$  thin films, spray pyrolysis.

<https://doi.org/10.15407/spqeo28.03.292>

PACS 81.15.Rs, 82.30.Lp, 88.40.hj, 88.40.jn

Manuscript received 31.01.25; revised version received 05.06.25; accepted for publication 03.09.25; published online 24.09.25.

### 1. Introduction

Photovoltaic (PV) cells are solar cells that directly convert sunlight into electricity and offer a clean and renewable source of energy. PV cells are typically constructed of semiconductor materials, namely silicon, to absorb photons and form electron-hole pairs. When light is incident, electrons are excited to higher energy levels, which produces an electric field inducing current flow [1]. PV cells can be constructed from various materials and processes and are continuously researched to enhance efficiency and reduce production costs. Thin-film solar cells employ transparent conductive oxide (TCO) layers, namely fluorine-doped tin oxide (FTO), that are optically transparent but facilitate the transport of charge carriers. Among the numerous materials considered for thin-film solar cells, the chalcogenide  $\text{Cu}_2\text{ZnSnS}_4$  (CZTS) has been of tremendous interest as an active layer. CZTS is a *p*-type semiconductor with a high optical absorption coefficient ( $\geq 10^4 \text{ cm}^{-1}$ ) and an ideal bandgap of approximately 1.5 eV [2]. However, its true efficiency in practical applications is limited by a huge open-circuit voltage ( $V_{oc}$ ) deficit relative to the Shockley–Queisser limit [3, 4]. A number of studies have attributed this efficiency limitation to Cu-Zn antistite defects, which are regarded as the most significant for further performance improvement [5]. To mitigate this issue, scientists attempted partial or total substitution of

transition metals and formed compounds of the type  $\text{Cu}_2\text{XSnS}_4$  ( $\text{X} = \text{Co}, \text{Fe}, \text{Ni}, \text{Mn}, \text{etc.}$ ). These compounds have already been found to possess new optoelectronic properties and are under investigation for multifunctional applications [6]. Specifically,  $\text{Cu}_2\text{CoSnS}_4$  (CCTS) thin films have been of special interest as potential absorber layers for PV cells due to their high visible and near-infrared absorption and direct bandgap of approximately 1.5 eV. Different deposition techniques for nanostructured CCTS thin films have been reported. Recent studies have highlighted the fact that nanostructuring can significantly improve the performance of CCTS by enhancing light absorption, charge carrier behavior, and interface quality.

High surface-to-volume ratio in nanostructured materials enables the physical and chemical properties to be controlled by shaping and sizing the particles. Nanostructured materials can be created through various physical and chemical processes. Additionally, the deposition method also plays an important role in controlling material performance, quality, and production costs. Various techniques have been investigated for the synthesis of CCTS thin films, including spray pyrolysis [7, 8], electrodeposition [9–13], thermal evaporation [14], green synthesis [15], spin coating [6], and sol-gel processes [16]. Among the mentioned methods, chemical spray pyrolysis (CSP) is a scale-up, low-cost, and reproducible process with the added advantage of mass pro-

duction of nanomaterials with fair reproducibility. CSP has been employed successfully for depositing various forms of nanopowders, 3D nanostructured films, and thin films, which have been applied in solar cells, sensors, energy storage devices, and bio applications [17–24].

TCO materials are of great interest in research due to their exceptional optoelectronic properties. Thin film solar cells (TFSCs) include TCO thin films to transmit the light onto absorber layers and as electrode materials to transport the charges away from the absorber layers. FTO thin films play the role of TCO in our study. FTO allows the incident light to pass through it towards the light-absorbing material. Moreover, FTO thin films are also beneficial for making the Ohmic contact with the light-absorbing layers and transporting the charge carriers. The deposited FTO thin films are utilized as conducting electrodes to investigate the photoactive nature of the CCTS absorber. CCTS is a *p*-type semiconductor analogous to  $\text{Cu}_2\text{ZnSnS}_4$  with an optical band gap between 1.46 and 1.61 eV. The direct band gap reduces the amount of material needed for fabricating efficient solar cells compared to other indirect band gap materials, namely, the crystalline silicon [25]. In our previous work [26], we explained the effect of substrate temperature (250 °C to 400 °C) on the properties of CCTS thin films prepared with a thiourea concentration of 1:5 for cations. The CCTS films at 350 °C exhibited 1.78% efficiency in photoelectron-chemical (PEC) solar cells. In this work, we are reporting the effect of thiourea concentration on the properties of CCTS thin films. This work aims at the utilization of an indigenously designed chemical spray pyrolysis set-up to deposit FTO thin films and CCTS thin films and the evaluation of their structural, morphological, and optical properties.

## 2. Materials and methods

The spray setup used in this study consists of a DC motor-driven nozzle assembly. The temperature controller comprises an Arduino microcontroller with a MAX-6675 thermocouple for accurate temperature sensing and a relay-controlled heater for automated regulation. A 16 X 2 LCD provides real-time monitoring of the temperature.

### 2.1. Experimental details

#### 2.1.1. Deposition of FTO and CCTS thin films

For the preparation of FTO thin film, the precursors used were  $\text{SnCl}_4 \cdot 5\text{H}_2\text{O}$ , and fluorine doping was achieved by  $\text{NH}_4\text{F}$ . The precursor solution for the deposition of FTO thin film was prepared by mixing  $\text{NH}_4\text{F}$  solution with  $\text{SnCl}_4 \cdot 5\text{H}_2\text{O}$  solution. The final molarities of ‘Sn’ and ‘F’ in the precursor solution were 0.47 M and 2.25 M, respectively. The pH of the resulting solution was equal to 1. 60 ml of the precursor solution was sprayed with a flow rate of 6 ml/min onto soda-lime glass substrates, which were preheated to a temperature of 450 °C.

For the deposition of CCTS thin films, the sources of copper, cobalt, tin, sulfur were 0.05 M  $\text{CuCl}_2 \cdot 2\text{H}_2\text{O}$ , 0.025 M  $\text{CoCl}_2 \cdot 6\text{H}_2\text{O}$ , 0.025 M  $\text{SnCl}_4 \cdot 5\text{H}_2\text{O}$  and  $\text{CH}_4\text{N}_2\text{S}$ , respectively. The ratio of cations (Cu+Co+Sn) and anions

(S) in the precursor solution was 1:7. The CCTS thin films were deposited at a substrate temperature of 350 °C. The 80 ml of precursor solution with methanol as a solvent was sprayed onto preheated substrates with a flow rate of 5 ml/min. After deposition, the samples were cooled naturally and investigated using various techniques. The PEC cells based on CCTS thin films with a thiourea concentration of 1:7 for cations provided an efficiency of 2.33%.

#### 2.1.2. Characterizations

The thickness measurements of the films were carried out using a surface profiler (Ambios, XP-I stylus profiler, USA). The FTO thin films sheet resistance is measured with a digital multimeter (RISH Multi, 12 S, India). X-ray diffractometer (Bruker D2 Phaser, USA) operated at 40 kV, 30 mA with  $\text{CuK}_\alpha$  radiation ( $\lambda = 1.5406 \text{ \AA}$ ) was used to study the structural properties of the deposited films. The surface morphology of the films was investigated using a MIRA 3, FE-SEM microscope equipped with an EDS detector (TESCAN, Czech Republic). UV-visible absorbance spectra of the films were recorded using a UV-visible spectrophotometer (UV 1800, Shimadzu, Japan). The photoactivity of CCTS films was investigated using the potentiostat PGSTAT302N (Metrohm Autolab, Netherlands). The PEC solar cell is fabricated with the structure: CCTS (working electrode) /  $\text{Na}_2\text{SO}_4$  (electrolyte) / platinum coated FTO (counter electrode). A 500 W tungsten lamp with an intensity of  $60 \text{ mW/cm}^2$  is utilized as a light source for photoelectrochemical measurements.

## 3. Results and discussion

The thickness of the FTO film was found to be 530 nm. The sheet resistance ( $R_s$ ) value of the FTO thin films varies from 8 to 42 Ohm/square. The thickness of spray-deposited CCTS films was found to be 383 nm.

Fig. 1a shows the XRD pattern of the FTO thin film deposited at a substrate temperature of 450 °C.

The weak reflexes attributed to (110), (101), (211), (310), and (301) planes are observed at  $26.50^\circ$ ,  $33.84^\circ$ ,  $51.72^\circ$ ,  $61.75^\circ$ , and  $65.70^\circ$ , respectively. The strong reflex attributed to the (200) plane is observed at a diffraction angle of  $37.95^\circ$ . The spray-deposited FTO thin film is polycrystalline and shows a preferred orientation along the (200) plane. The XRD pattern confirmed that the spray-deposited FTO thin film exhibits a tetragonal structure compared to the standard JCPDS card – 00-021-1250 of  $\text{SnO}_2$  [27].

Fig. 1b shows the XRD pattern of CCTS films. The strong reflex of (112) plane is observed at  $28.64^\circ$ . The stannite structure of the films is confirmed by comparing XRD patterns with the standard JCPDS Card no. 00-026-0513 [28].

The crystallite sizes (*D*) of FTO and CCTS thin films are calculated using Eq. (1) [29]

$$D = \frac{k\lambda}{\beta \cos \theta} \quad (1)$$

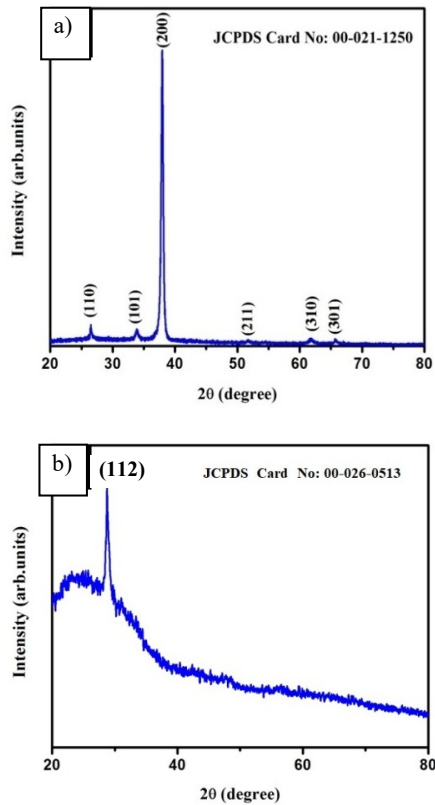


**Fig. 1.** XRD patterns of (a) FTO thin film deposited at a substrate temperature of 450 °C and (b) CCTS thin film.

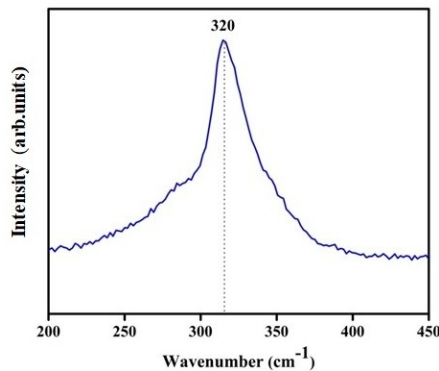


**Fig. 2.** Raman spectrum of CCTS thin film.

where  $k$  is the shape factor (usually taken as 0.9 for spherical crystallites),  $\lambda$  is the wavelength of the X-ray used,  $\beta$  is the FWHM (full width at half maximum), and  $\theta$  is Bragg's angle of diffraction. The crystallite sizes of 24.55, 14.63, 20.64, 17.90, 13.45, and 22.29 nm were observed along (110), (101), (200), (211), (310), and (301) reflexes. The average crystallite size for FTO thin film is 18.91 nm. The crystallite size along (112) plane for CCTS thin film is 16.81 nm. The structural parameters of FTO and CCTS thin films obtained using XRD data are represented in Table 1.

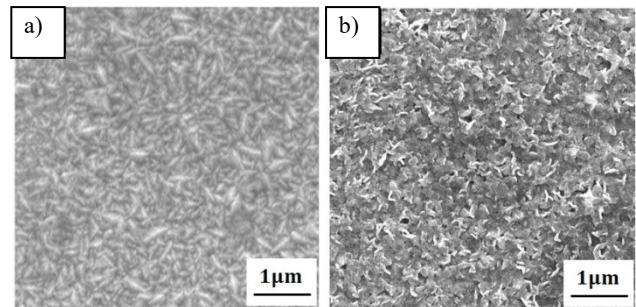
The comparison of FTO thin films in this work with other research groups based on substrate temperature,

surface morphology, crystallite size/ grain size, and preferential orientation is summarized in Table 2.

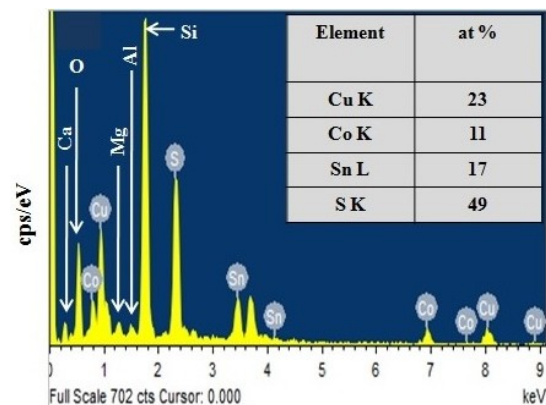
XRD patterns of secondary phases, namely  $\text{Cu}_2\text{SnS}_3$  (CTS) and CCTS, show close resemblance, which limits the discrimination of CTS and CCTS structures using only X-ray diffraction data. Therefore, Raman analysis is carried out to confirm the phase purity of spray-deposited CCTS thin films. Fig. 2 shows a typical 200...450  $\text{cm}^{-1}$  Raman spectrum of CCTS thin films deposited at 350 °C for a 1:7 thiourea concentration. The most intense peak is observed at 320  $\text{cm}^{-1}$ , which can be assigned to the symmetry mode  $A_1$ . It is mainly due to vibrations of S anions. The peak appearing at 350  $\text{cm}^{-1}$  in the Raman spectrum of CCTS represents the existence of metal polysulfide impurities of the types  $\text{SnS}_2$  and  $\text{CuCoS}_2$  [35]. As no such intense peak is appearing in the Raman spectrum of the spray-coated CCTS thin films, this signifies phase purity of the deposited material.

Fig. 3a shows an FE-SEM image of an FTO thin film deposited at a substrate temperature of 450 °C. One can see that the surface of the film is covered by densely packed grains, free from voids, and homogeneous.

The surface morphology of CCTS thin film is shown in Fig. 3b. One can see a flake-like surface morphology, which seems uniform and compact. The EDS spectrum of CCTS thin film deposited at a substrate temperature of 350 °C is shown in Fig. 4.



**Fig. 3.** FE-SEM micrographs at  $\times 25,000$  magnification of Microscope (a) FTO film deposited at 450 °C (b) CCTS thin film deposited at 350 °C.



**Fig. 4.** EDS spectrum of CCTS thin film deposited at 350 °C. The composition ratio of Cu:Co:Sn:S is 2.09:1:1.54:4.45, whereas the ratio of S:(Cu+Co+Sn) is 0.96.

**Table 1.** The structural parameters of FTO and CCTS thin films.

Material	Substrate temperature (°C)	Miller indices ( <i>hkl</i> )	Standard diffraction angle (2 $\theta$ )°	Observed diffraction angle (2 $\theta$ )°	Calculated <i>d</i> (Å)	FWHM (rad)	Crystallite size <i>D</i> (nm)
FTO	450	(110)	26.57	26.5	3.36	0.0058	24.55
		(101)	33.87	33.84	2.64	0.0099	14.63
		(200)	37.95	37.95	2.36	0.0071	20.64
		(211)	51.75	51.72	1.76	0.0086	17.90
		(310)	61.89	61.75	1.50	0.012	13.45
		(301)	65.96	65.7	1.42	0.0074	22.29
CCTS	350	(112)	28.56	28.64	3.11	0.008	16.81

**Table 2.** Comparison of FTO thin films in this work with other research groups based on substrate temperature, surface morphology, crystallite size/ grain size, and preferential orientation.

Substrate temperature (°C)	Surface morphology	Crystallite size /grain size (nm)	Preferential orientation	Crystal structure	Ref.
350–500	Dense, compact, uniform grains	~190	(200)	Tetragonal	[30]
400–500	Fine-grained, compact, improved with doping	50–150	(200), varies with doping	Tetragonal	[31]
~400	Granular; roughness increases post-treatment	~140	(110), (200)	Tetragonal	[32]
450–550	Rough, high haze for enhanced light scattering	Not reported	Not emphasized	Tetragonal	[33]
300–550	Columnar at high temperature; denser morphology at low temperature	20–200	(200)	Tetragonal	[34]
450	Dense and compact	18.91	(200)	Tetragonal	This work

**Table 3.** Comparison of CCTS and other quaternary semiconductors.

Material	Deposition conditions	Surface morphology	Optical properties	Ref.
Cu <sub>2</sub> NiSnS <sub>4</sub> (CNTS)	Potentiostatic electrodeposition at –0.98 V vs. Ag/AgCl; aqueous solution with Cu <sup>2+</sup> , Ni <sup>2+</sup> , Sn <sup>2+</sup> , and S <sub>2</sub> O <sub>3</sub> <sup>2–</sup> ; sulfurization at 500 °C	Compact microsheet morphology with homogeneous texture	Band gap ~1.6 eV; suitable for PV	[36]
Cu <sub>2</sub> FeSnS <sub>4</sub> (CFTS)	Electrodeposition at –0.9 V vs Ag/AgCl; Fe <sup>2+</sup> concentration varied; sulfurization at 450 °C	Dense and compact; morphology depends on ‘Fe’ content	Band gap ~1.5 eV; good for PV	[37]
Cu <sub>2</sub> CoSnS <sub>4</sub> (CCTS)	Pulsed electrodeposition with/without additives; annealing at 500 °C in sulfur atmosphere	Uniform films; additives improve crystallinity	Band gap ~1.5 eV; promising PV use	[10]
Cu <sub>2</sub> CoSnS <sub>4</sub> (CCTS)	Spray pyrolysis	Flake-like, dense	1.53 eV	Present work

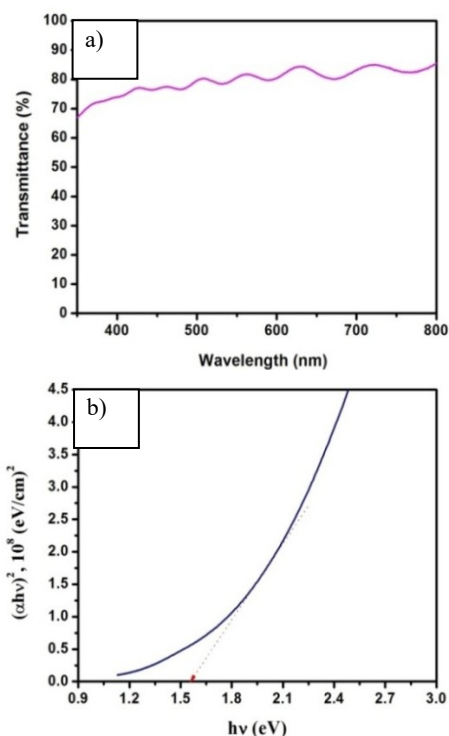


**Fig. 5.** (a) Transmittance spectrum of FTO film deposited at 450 °C, (b) plot of  $(\alpha h\nu)^2$  vs photon energy ( $h\nu$ ) of CCTS thin film deposited at 350 °C.

Fig. 5a shows the transmittance of the FTO film deposited at a substrate temperature of 450 °C. The transmittance of FTO thin film is more than 75% within the range 400...800 nm. Fig. 5b shows the plot of  $(\alpha h\nu)^2$  vs photon energy ( $h\nu$ ) of CCTS thin film deposited at 350 °C.

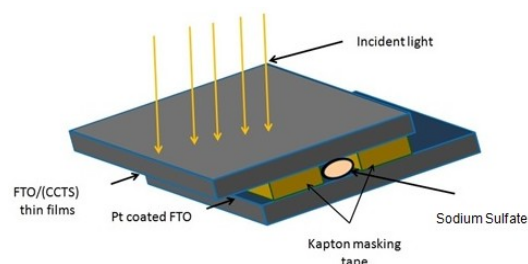


**Fig. 6.** Scheme of PEC solar cells fabricated with CCTS films.

The optical band gap of CCTS thin film (1.53 eV) is obtained by extrapolating the linear portion of the plots  $(\alpha h\nu)^2$  vs photon energy ( $h\nu$ ) at  $\alpha = 0$ . The comparison of physical properties of CCTS and other quaternary semiconductors reported by other research groups is summarized in Table 3.

Fig. 6 shows the scheme of PEC solar cells fabricated with CCTS films.

Fig. 7 shows the current density-voltage ( $J$ - $V$ ) characteristic of the CCTS thin film-based PEC solar cell under illumination.

The fill factor (FF) of the PEC solar cells and power conversion efficiency ( $\eta$  %) are evaluated using Eqs. (2) and (3) [38–40]:

$$FF = \frac{J_{\max} \times V_{\max}}{J_{sc} \times V_{oc}}, \quad (2)$$

$$\eta = \frac{J_{sc} \times V_{oc}}{P_{in}} \times FF \times 100, \quad (3)$$

where  $V_{oc}$  is the open circuit voltage,  $J_{sc}$  – short-circuit current density,  $V_{\max}$  – maximum voltage,  $J_{\max}$  – maximum current density,  $FF$  – fill factor, and  $P_{in}$  – input power density of the incident light.

**Table 4.** The PEC performance parameters of CCTS thin film deposited at an optimized substrate temperature of 350 °C.

Material	$J_{sc}$ ( $\mu\text{A}/\text{cm}^2$ )	$V_{oc}$ (mV)	$J_{\max}$ ( $\mu\text{A}/\text{cm}^2$ )	$V_{\max}$ (mV)	FF	Efficiency ( $\eta$ )%
CCTS	29	151	17	82	0.32	2.33

**Table 5.** Comparison of the studied spray-deposited CCTS thin films with those reported by other research groups.

Synthesis temperature	Solvent	Surface morphology	Energy bandgap (eV)	Photoactivity study	Ref.
300 °C	double-distilled water	homogeneous	1.41–1.12 changing with film thickness	–	[41]
(400 ± 10) °C	aqueous solution	irregular particle size	1.3–1.85	–	[42]
200 °C, deposited films were annealed in the sulfur atmosphere at 550 °C for 30 min	deionized water	granular and rough	1.72	–	[43]
280–360 °C	distilled water	granular, rough, and compact	1.75 for a substrate temperature of 320 °C	–	[44]
350 °C	methanol	flake-like, uniform, and compact	1.53	PEC cell provided 2.33% power conversion efficiency	This work

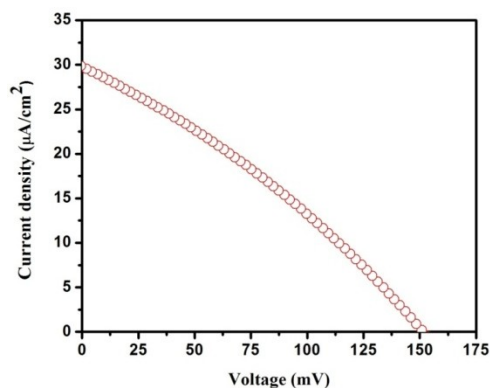


**Fig. 7.** The current density-voltage ( $J$ - $V$ ) characteristic of the CCTS thin film.

Table 4 summarizes the PEC performance parameters of CCTS thin film deposited at an optimized substrate temperature of 350 °C. The PEC solar cell exhibits a power conversion efficiency of 2.33%.

The comparison of spray-coated CCTS thin films from this work with those reported by other research groups, concerning substrate temperature, surface morphology, optical energy bandgap, and photoactivity, is summarized in Table 5.

#### 4. Conclusions

The XRD study of FTO thin films deposited by CSP confirmed their tetragonal structure. The optical study revealed that they exhibit transmittance higher than 75% within the range 400...800 nm. The sheet resistance of the studied FTO films ranges from 8 to 42 Ohm/square. These FTO thin films have been utilized as conducting electrodes for depositing CCTS thin films. The XRD study of CCTS thin films fabricated with a 1:7 thiourea concentration provided a tetragonal crystal structure with preferred orientation along the (112) plane. The study of surface morphology revealed a compact flake-like morphology. The EDS analysis revealed the presence of Cu, Co, Sn, and S as the constituent elements in the deposited films. Among the tested conditions, the film synthesized at 350 °C with methanol as the solvent showed the best performance, exhibiting a uniform, flake-like morphology, a moderate bandgap (1.53 eV), and a notable power conversion efficiency of 2.33% for the PEC solar cells fabricated with CCTS thin films with a 1:7 thiourea concentration. In contrast, films made with aqueous solvents at other temperatures had rougher morphologies, inconsistent bandgap, and no photoactivity. These findings emphasize the importance of solvent selection and synthesis temperature in optimizing CCTS films for photovoltaic applications.

The present investigation offers a cost-effective approach to the fabrication of TFSCs.

#### Conflicts of interest

The authors declare no conflicts of interest regarding the publication of this paper.

#### Funding sources

This research did not receive a specific grant from funding agencies in the public, commercial, or not-for-profit sectors.

#### Data availability statement

The datasets analyzed during the present study are available from the corresponding author upon reasonable request.

#### References

1. Jordehi A.R. Parameter estimation of solar photo-voltaic (PV) cells: A review. *Renew. Sustain. Energy Rev.* 2016. **61**. P. 354–371. <https://doi.org/10.1016/j.rser.2016.03.049>.
2. Khalate S., Kate R., Kim J. *et al.* Effect of depo-sition temperature on the properties of  $\text{Cu}_2\text{ZnSnS}_4$  (CZTS) thin films. *Superlattices Microstruct.* 2017. **103**. P. 335–342. <https://doi.org/10.1016/j.spmi.2017.02.003>.
3. Bourdais S., Choné C., Delatouche B. *et al.* Is the Cu/Zn disorder the main culprit for the voltage deficit in kesterite solar cells? *Adv. Energy Mater.* 2016. **6**, No 12. P. 1502276. <https://doi.org/10.1002/aenm.201502276>.
4. He M., Yan C., Li J. *et al.* Kesterite solar cells: insights into current strategies and challenges. *Adv. Sci.* 2021. **8**, No 9. P. 2004313. <https://doi.org/10.1002/advs.202004313>.
5. Kangsabanik M., Gayen R.N. A comprehensive review on the recent strategy of cation substitution in CZTS (Se) thin films to achieve highly efficient kesterite solar cells. *Sol. RRL.* 2023. **7**. P. 2300670. <https://doi.org/10.1002/solr.202300670>.
6. Krishnaiah M., Mishra R.K., Seo S.G. *et al.* Highly crystalline, large grain  $\text{Cu}_2\text{CoSnS}_4$  films with reproducible stoichiometry via direct solution spin coating for optoelectronic device application. *Ceram. Int.* 2019. **45**, No 9. P. 12399–12405. <https://doi.org/10.1016/j.ceramint.2019.03.167>.
7. El Khouja O., Assahsahi I., Nouneh K. *et al.* Structural and transport properties of  $\text{Cu}_2\text{CoSnS}_4$  films prepared by spray pyrolysis. *Ceram. Int.* 2022. **48**, No 21. P. 32418–32426. <https://doi.org/10.1016/j.ceramint.2022.07.185>.
8. Sivagami D., Priyadarshini B.G. Role of carbon quantum dot for enhanced performance of photo-absorption in  $\text{Cu}_2\text{CoSnS}_4$  superstrate solar cell device. *Mater. Adv.* 2022. **3**. P. 2405–2416. <https://doi.org/10.1039/D1MA01117K>.
9. Ait Layachi O., Moujib A., El Khouja O. *et al.* Electrodeposition mechanism of  $\text{Cu}_2\text{CoSnS}_4$  thin films onto FTO-coated glass: Effect of some additives. *J. Electroanal. Chem.* 2024. **959**. P. 118177. <https://doi.org/10.1016/j.jelechem.2024.118177>.
10. Ait Layachi O., Boudouma A., Lasri M. *et al.* Pulsed potential co-electrodeposition of  $\text{Cu}_2\text{CoSnS}_4$  absorber layer on fluorinated tin oxide (FTO)-coated glass. *J. Appl. Electrochem.* 2024. **54**, No 12. P. 2745–2756. <https://doi.org/10.1007/s10800-024-02131-x>.
11. Oubakalla M., Beraich M., Taibi M. *et al.* Effects of copper concentration on the properties of  $\text{Cu}_2\text{CoSnS}_4$  thin films co-electrodeposited on the FTO substrate. *J. Mater. Sci.: Mater. Electron.*



2022. **33**, No 15. P. 12016–12025. <https://doi.org/10.1007/s10854-022-08162-4>.
12. Boudouma A., Ait Layachi O., Hrir H. *et al.* Electrodeposition synthesis of  $\text{Cu}_2\text{ZnSnS}_4$  (CZTS) thin films as a promising material for photovoltaic cells: fundamentals, methods, and future prospects – A comprehensive review. *Mater. Today Sustain.* 2024. **28**. <https://doi.org/10.1016/j.mtsust.2024.101018>.
13. Beraich M., Taibi M., Guenbour A. *et al.* Preparation and characterization of  $\text{Cu}_2\text{CoSnS}_4$  thin films for solar cells via co-electrodeposition technique: Effect of electrodeposition time. *Optik.* 2019. **193**. P. 162996. <https://doi.org/10.1016/j.ijleo.2019.162996>.
14. Hammami H., Marzougui M., Oueslati H. *et al.* Synthesis, growth and characterization of  $\text{Cu}_2\text{CoSnS}_4$  thin films via thermal evaporation method. *Optik.* 2021. **227**. P. 166054. <https://doi.org/10.1016/j.ijleo.2020.166054>.
15. Ivakhno-Tshehnyk O., Selyshchev O., Kondratenko S. *et al.* “Green” aqueous synthesis, structural, and optical properties of quaternary  $\text{Cu}_2\text{ZnSnS}_4$  and  $\text{Cu}_2\text{NiSnS}_4$  nanocrystals. *phys. status solidi (b)*. 2024. P. 2400203. <https://doi.org/10.1002/pssb.202400203>.
16. El kissani A., Ait elhaj D., Drissi S. *et al.* Structural, optical and electrical properties of  $\text{Cu}_2\text{CoSnS}_4$  thin film solar cells prepared by facile sol-gel route. *Thin Solid Films.* 2022. **758**. 139430. <https://doi.org/10.1016/j.tsf.2022.139430>.
17. Zeng X., Tai K., Zhang T. *et al.*  $\text{Cu}_2\text{ZnSn}(\text{S}, \text{Se})_4$  kesterite solar cell with 5.1% efficiency using spray pyrolysis of aqueous precursor solution followed by selenization. *Sol. Energy Mater. Sol. Cells.* 2014. **124**. P. 55. <https://doi.org/10.1016/j.solmat.2014.01.029>.
18. Theresa T., Mathew M., Kartha C.S. *et al.*  $\text{CuInS}_2/\text{In}_2\text{S}_3$  thin film solar cell using spray pyrolysis technique having 9.5% efficiency. *Sol. Energy Mater. Sol. Cells.* 2005. **89**. P. 27–36. <https://doi.org/10.1016/j.solmat.2004.12.005>.
19. Kärber E., Abass A., Khelifi S. *et al.* Electrical characterization of all-layers-sprayed solar cell based on ZnO nanorods and extremely thin CIS absorber. *Sol. Energy.* 2013. **91**. P. 48–58. <https://doi.org/10.1016/j.solener.2013.01.020>.
20. Sahm T., Mädler L., Gurlo A. *et al.* Flame spray synthesis of tin dioxide nanoparticles for gas sensing. *Sens. Actuators B: Chem.* 2004. **98**. P. 148–153. <https://doi.org/10.1016/j.snb.2003.10.003>.
21. Ghimbeu C., Schoonman J., Lumbreras M., Siadat M. Electrostatic spray deposited zinc oxide films for gas sensor applications. *Appl. Surf. Sci.* 2007. **253**. P. 7483. <https://doi.org/10.1016/j.apsusc.2007.03.039>.
22. Karthick S., Gnanakan S., Subramania A., Kim H. Nanocrystalline  $\text{LiMn}_2\text{O}_4$  thin film cathode material prepared by polymer spray pyrolysis method for Li-ion battery. *J. Alloys Compd.* 2010. **489**. P. 674–677. <https://doi.org/10.1016/j.jallcom.2009.09.147>.
23. Tartaj P., Morales M., Gonzalez-Carreño T., Serna C. Advances in magnetic nanoparticles for biotechnology applications. *J. Magn. Magn. Mater.* 2005. **290–291**. P. 28–34. <https://doi.org/10.1016/j.jmmm.2004.11.155>.
24. Tartaj P., Morales M.P., Veintemillas-Verdaguer S. *et al.* The preparation of magnetic nanoparticles for applications in biomedicine. *J. Phys. D: Appl. Phys.* 2003. **36**. P. R181. <https://doi.org/10.1088/0022-3727/36/13/202>.
25. Xie Y., Zhang C., Yang G. *et al.* Highly crystalline stannite-phase  $\text{Cu}_2\text{XSnS}_4$  (X = Mn, Fe, Co, Ni, Zn and Cd) nanoflower counter electrodes for ZnO-based dye-sensitized solar cells. *J. Alloys Compd.* 2017. **696**. P. 938–946. <https://doi.org/10.1016/j.jallcom.2016.12.043>.
26. Maldar P., Gaikwad M., Mane A. *et al.* Fabrication of  $\text{Cu}_2\text{CoSnS}_4$  thin films by a facile spray pyrolysis for photovoltaic application. *Solar Energy.* 2017. **158**. P. 89–99. <https://doi.org/10.1016/j.solener.2017.09.036>.
27. Swanson H.E., Tatge E. Standard x-ray diffraction powder patterns. *National Bureau of Standards (US), Circular 539, Volume I.* 1953.
28. Schfifer W., Nitsche R. Tetrahedral quaternary chalcogenides of the type  $\text{Cu}_2\text{-II-IV-S}_4$  ( $\text{Se}_4$ ). *Mater. Res. Bull.* 1974. **9**. P. 645–654. [https://doi.org/10.1016/0025-5408\(74\)90135-4](https://doi.org/10.1016/0025-5408(74)90135-4).
29. Mane A.A., Moholkar A.V. Effect of solution concentration on physicochemical and  $\text{NO}_2$  gas sensing properties of sprayed  $\text{MoO}_3$  nanobelts. *Thin Solid Films.* 2018. **648**. P. 50–61. <https://doi.org/10.1016/j.tsf.2018.01.008>.
30. Abd-Lefdil M., Diaz R., Bihri H. *et al.* Preparation and characterization of sprayed FTO thin films. *Eur. Phys. J. Appl. Phys.* 2007. **38**. P. 217–219. <https://doi.org/10.1051/epjap:2007090>.
31. Moulik S.R., Ghatak A., Ghosh B. Study of surface chemistry and microstructure of  $\text{TiO}_2$  nanostructures on Pt(111)/Si wafer and FTO glass substrates: a comparative approach. *Surf. Sci.* 2016. **651**. P. 175–181. <https://doi.org/10.1016/j.susc.2016.04.011>.
32. Ramaiah K., Raja V. Structural and electrical properties of fluorine doped tin oxide films prepared by spray-pyrolysis technique. *Appl. Surf. Sci.* 2006. **253**. P. 1451. <https://doi.org/10.1016/j.apsusc.2006.02.019>.
33. Adnane M., Cachet H., Folcher G., Hamzaoui S. Beneficial effects of hydrogen peroxide on growth, structural and electrical properties of sprayed fluorine-doped  $\text{SnO}_2$  films. *Thin Solid Films.* 2005. **492**. P. 240–247. <https://doi.org/10.1016/j.tsf.2005.06.085>.
34. Moholkar A.V. *et al.* Solvent-dependent growth of sprayed FTO thin films with mat-like morphology. *Sol. Energy Mater. Sol. Cells.* 2008. **92**. P. 1439–1444. <https://doi.org/10.1016/j.solmat.2008.06.010>.
35. López-Vergara F., Galdámez A., Manríquez V. Electrical behavior of a  $\text{Cu}_2\text{Fe}_{0.4}\text{Co}_{0.6}\text{SnS}_4$  ceramic. *J. Chil. Chem. Soc.* 2013. **4**. P. 2131–2135. <http://doi.org/10.4067/S0717-97072013000400051>.
36. Ait Layachi O., Hrir H., Boudouma A. *et al.* Electrodeposition of  $\text{Cu}_2\text{NiSnS}_4$  absorber layer on FTO substrate for solar cell applications. *RSC Adv.* 2024. **14**. P. 29439. <https://doi.org/10.1039/D4RA04249B>.
37. Ait Layachi O., Boudouma A., Hrir H. *et al.* Electrodeposition of  $\text{Cu}_2\text{FeSnS}_4$  thin films for solar cell applications: mechanism of deposition and influence of  $\text{Fe}^{2+}$  concentration. *J. Solid State Electrochem.* 2024. **28**. P. 2345–2358. <https://doi.org/10.1007/s10008-024-06060-9>.

38. Gudage Y.G., Sharma R. Growth kinetics and photoelectrochemical (PEC) performance of cadmium selenide thin films: pH and substrate effect. *Curr. Appl. Phys.* 2010. **10**. P. 1062–1070. <https://doi.org/10.1016/j.cap.2009.12.043>.
39. Hussain S., Cao C., Usman Z. *et al.* Effect of films morphology on the performance of Cu<sub>2</sub>O PEC solar cells. *Optik*. 2018. **172**. P. 72–78. <https://doi.org/10.1016/j.ijleo.2018.07.026>.
40. Maldar P.S. *et al.* Spray deposited Cu<sub>2</sub>CoSnS<sub>4</sub> thin films for photovoltaic application: Effect of film thickness. *Thin Solid Films*. 2020. **709**. P. 138236. <https://doi.org/10.1016/j.tsf.2020.138236>.
41. Al-Zahrani H.Y.S. Synthesis, optical and optoelectrical analysis of the Cu<sub>2</sub>CoSnS<sub>4</sub> thin films as absorber layer for thin-film solar cells. *J. Mater. Sci.: Mater. Electron.* 2020. **31**. P. 6900–6909. <https://doi.org/10.1007/s10854-020-03252-7>.
42. Ahmed M.A., Bakr N.A., Kamil A.A. Synthesis and characterization of chemically sprayed Cu<sub>2</sub>CoSnS<sub>4</sub> thin films. *Chalcogenide Lett.* 2019. **16**. P. 231–239.
43. Bargaoui I., Bitri N., Dridi S., Ly I. Cu<sub>2</sub>CoSnS<sub>4</sub> thin films as suitable absorber layers for photovoltaic applications, synthesized by spray pyrolysis. *Mater. Res. Express*. 2019. **6**. P. 086410. <https://doi.org/10.1088/2053-1591/ab1d29>.
44. Harrathi F., Aubry E., Dridi S. *et al.* Effect of the substrate temperature on the synthesis of the Cu<sub>2</sub>CoSnS<sub>4</sub> thin films by spray pyrolysis for solar cells devices. *J. Mater. Sci.: Mater. Electron.* 2023. **34**. P. 304. <https://doi.org/10.1007/s10854-022-09720-6>.

#### Authors' contributions

**Maldar P.S.:** conceptualization, methodology, formal analysis, investigation, data curation (partially), writing – original draft, visualization, writing – review & editing.

**Pusawale S.N.:** conceptualization, methodology, writing – original draft, writing – review & editing.

**Tambat A.S.:** validation, formal analysis, investigation, resources, data curation.

#### Authors and CV



**P.S. Maldar**, Ph.D. in Physics (Science and Technology, 2019), Assistant Professor of Physics in the Department of Sciences and Humanities at the Rajarambapu Institute of Technology, affiliated to Shivaji University Kolhapur. Authored more than 15 research scientific papers, 2 Indian patents. His current areas of interest are hetero-junction solar cells, dye-sensitized solar cells, preparation of cost-efficient counter electrodes based on metal sulfide thin films, photocatalysis, and nanoparticle synthesis for energy storage and conversion. E-mail: [parvejha.maldar@ritindia.edu](mailto:parvejha.maldar@ritindia.edu), <https://orcid.org/0000-0003-4573-2478>



**Swati N. Pusawale**, Ph.D. in Physics (2011), Assistant Professor at the Department of Sciences and Humanities, Rajarambapu Institute of Technology, affiliated to Shivaji University Kolhapur. Author of over 20 research publications. The area of her scientific interests includes the synthesis of nanomaterials and their application in energy storage devices. E-mail: [swati.pusawale@ritindia.edu](mailto:swati.pusawale@ritindia.edu)



**A.S. Tambat**, completed his M.Sc. in Physics in 2022 with a specialization in Solid State Physics from Shivaji University (M.S.) India. His M.Sc. project was on synthesizing manganese oxide thin films by the SILAR method. Currently, he is working as

Assistant Professor in Physics at the Department of Sciences and Humanities, Rajarambapu Institute of Technology, affiliated to Shivaji University Kolhapur. His research area includes nanomaterial synthesis for energy storage and conversion. E-mail: [ajay.tambat@ritindia.edu](mailto:ajay.tambat@ritindia.edu)

#### Дослідження фотоелектрохімічної дії тонких плівок Cu<sub>2</sub>CoSnS<sub>4</sub>, нанесених розпиленням на підкладку FTO

**P.S. Maldar, S.N. Pusawale, A.S. Tambat**

**Анотація.** У цьому дослідженні представлено результати осадження тонких плівок оксиду олова, легованого фтором (FTO), які використовувалися як провідні електроди для осадження тонких плівок Cu<sub>2</sub>CoSnS<sub>4</sub> (CCTS), за допомогою власної розробленої установки спреї-піролізу. Тонкі плівки FTO та CCTS були осаджені методом хімічного піролізного розпилення. Тонкі плівки CCTS осаджувалися зі сталою кількістю розчину-прекурсора 80 мл шляхом зміни концентрації тіосечовини відносно катіонів у співвідношенні 1:7. Температура осадження була встановлена на рівні 350 °C для тонких плівок CCTS, а співвідношення катіонів до аніонів у розчині-прекурсорі становило 1:7. Отримані тонкі плівки CCTS досліджено методами рентгенівської дифракції, скануючої електронної мікроскопії та раманівської спектроскопії. Встановлено, що ефективність фотоелектрохімічних сонячних елементів, виготовлених з концентрацією тіосечовини 1:7 відносно катіонів, становить 2,33%.

**Ключові слова:** тонкі плівки FTO, тонкі плівки Cu<sub>2</sub>CoSnS<sub>4</sub>, піролізне розпилення, фотоелектрохімічний елемент.